Research Article

Exploring EPR Parameters of ^{99}Tc Complexes for Designing New MRI Probes: Coordination Environment, Solvent, and Thermal Effects on the Spectroscopic Properties

Bruna T. L. Pereira,[1] Érika Ferreira Silva,[1] Mateus A. Gonçalves,[1] Daiana T. Mancini,[1] and Teodorico C. Ramalho[1,2]

[1]*Department of Chemistry, Federal University of Lavras, P.O. Box 3037, 37200-000 Lavras, MG, Brazil*
[2]*Center for Basic and Applied Research, Faculty of Informatics and Management, University of Hradec Kralove, Hradec Kralove, Czech Republic*

Correspondence should be addressed to Teodorico C. Ramalho; teo@dqi.ufla.br

We have evaluated the solvent and thermal effects on spectroscopic parameters of ^{99}Tc complexes coordinated to explicit water molecules. Molecular dynamics simulations were performed followed by hyperfine coupling constant calculations (A_{iso}). Our results show a significant increase of A_{iso}, which demonstrates that the studied compounds can be promising contrast agents in MRI.

1. Introduction

Currently, cancer is one of the most serious health problems faced by humanity. Studies show a large increase in incidence of this disease, including a growing number of deaths [1]. Among the several types of cancer, breast cancer is the most frequent in the world, incidence being more common in women [2].

Generally, breast cancer is diagnosed in advanced stages and consequently presents the highest mortality rates in the entire world [2, 3]. However, more recently, some modern techniques, such as tomography and Magnetic Resonance Imaging (MRI) [4], which allow the diagnosis in early stages, have been utilized for breast cancer diagnosis. The MRI has been considered a very effective technique due its high sensitivity in finding small tumors and nodules in the breast [5]. In fact, MRI has been shown as a strong tool for early stage breast cancer diagnosis [5].

The MRI is considered a noninvasive technique for diagnosis and is based on the magnetic properties of the ^{1}H and ^{17}O nuclei, which are the most abundant elements in the human body [6]. However, with only the natural relaxation of the water molecules in the body, it is often not possible to obtain clear MRI images. Thus, aiming to improve the image resolution contrast agents (CAs) are used [7].

The CAs are paramagnetic compounds able to decrease longitudinal and transverse relaxation times of water molecules in the proximity of their structure, thus facilitating breast cancer diagnosis [8]. Based on this context, it is necessary to understand the relaxation mechanisms of water molecules and the influence of paramagnetic effects on the ^{1}H and ^{17}O hyperfine coupling constant (A_{iso}) values [7].

More recently, radioisotopes of technetium (Tc) have been considered promising nuclei for the NMR (Nuclear Magnetic Resonance) and MRI techniques [9–11]. Based on this context, in 2006 Tzanopoulou et al. synthesized the $(^{99m}\text{Tc})(\text{CO})_3(\text{NNO})$ complex conjugated to the antitumor agent 2-(4′-aminophenyl)benzothiazole [ABT; see Complex **1**, Figure 1] [12]. The ABT compound presents nanomolar activity in vitro against some breast cancer cells in humans. In addition, this compound can be utilized for transporting the radioisotope of choice to the diseased tissue, facilitating the diagnostic and therapeutic applications against breast cancer [13–15].
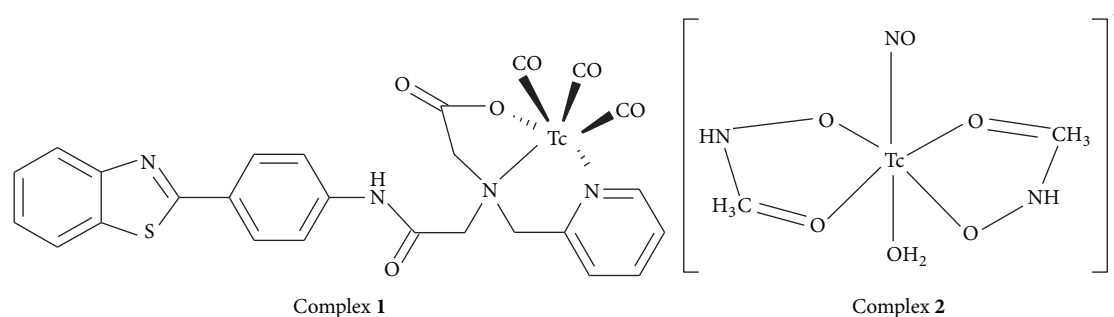
FIGURE 1: $(^{99m}Tc)(CO)_3(NNO)$ conjugated with 2-(4′-aminophenyl)benzothiazole**(1)**; oxotechnetium(V) complex with the ligand N(2(1-H-pyrolmethyl)N′-(4-pentene-3-one-2)ethane-1,2-diamine **(2)**.

The ^{99m}Tc is a metastable nucleus and emitter of gamma energy ($E\gamma$ = 140 keV), with a relatively short half-life ($t1/2$ = 6.02 h). The ^{99m}Tc disintegrates by emission of gamma radiation to yield ^{99}Tc, which is less toxic and more stable and presents a long half-life ($t_{1/2} = 2.2 \times 10^5$ years) [16]. The ^{99}Tc nuclei presents a quadrupole moment equal to -0.19×10^{-28} m^2 and a large spin, I = 9/2. It should be kept in mind that these characteristics can make of the ^{99}Tc a promising nucleus for the EPR (Electron Paramagnetic Resonance) spectroscopy and MRI studies [17, 18]. According to literature, the ^{99m}Tc complexes are used in 85% of cancer diagnosis cases in hospitals [19].

As another paramagnetic complex, $[Tc(NO)(aha)_2(H_2O)]^+$ (II) (Complex **2**, Figure 1) was used to evaluate the Tc coordination environment effect on the ^1H and ^{17}O hyperfine coupling constant (A_{iso}) values. The EPR parameters of a set of Tc(II) nitrosyl complexes were reported in the previous studies in the literature [20].

In order to validate our calculation strategy for ^1H and ^{17}O A_{iso} values, the complex $[Mn(H_2O)_6]^{2+}$ was used. Within this context, the goal of this work is to explore the spectroscopic properties of the $(^{99m}Tc)(CO)_3(NNO)$ complex conjugated with the ABT compound in solution, evaluating the thermal and solvent effects on the ^1H and ^{17}O hyperfine coupling constant values, and thus propose this compound as a new MRI contrast agent. In addition, different coordinating modes as well as solvent and thermal effects on A_{iso} values for Tc complexes were investigated.

2. Computational Methods

2.1. Optimization and Molecular Dynamics Procedure. Geometries were fully optimized using the gradient-corrected density functional BP86 [21–23] and LanL2dz basis set [24]. Water molecules were introduced in the system using the ADF (Amsterdam Density Functional) software [25], the solvent sphere had radius 15 Å, and the solute factor was approximately 1.0 Å. Since the time-scale accessible to the atom-centered density matrix propagation (ADMP) [25] method is very restricted, no extensive equilibration is possible and care must be taken to start from reasonably well preequilibrated configuration. To this end, we first prepared a classical system through an MD simulation using the modified force field

(GROMOS96) [26, 27] with the GROMACS 5.1 package [28]. As usual, periodic boundary conditions (PBC) and a cutoff distance of 9.0 Å were applied. Using the last configuration from classical MD as the starting point, we subsequently started quantum MD simulations using the ADMP method at the DFT level [25] (BP86/LanL2dz). These procedures have been employed with success in previous studies [11].

ADMP employs an extended Lagrangian similar to the well-known Car-Parrinello molecular dynamics. It can treat all electrons quantum-mechanically and can control the deviations from the Born-Oppenheimer surface precisely [25, 29]. In this work, a temperature of 310 K (physiologic temperature) was used throughout the simulation. In fact, this temperature is suitable to simulate the behavior of compounds in biological systems. After an equilibrium time of 1 ps, in which a temperature of 310 K was maintained via velocity rescaling, statistical averages and snapshots for hyperfine coupling constant (HFCC) calculations were collected from subsequent unconstrained micro canonical runs of 1 ps, obtaining a total of 1000 conformations. Snapshots were taken every 25 fs generating a total of 40 conformations [11] for use in HFCC calculations. A new method of selecting structures has been successfully used, OWSCA; this method uses the wavelet transform to decompose the DM signal; the signal decomposed by the transform is able to represent well and with a minimum error the entire DM signal [30]. All optimization and quantum MD calculations were carried out using Gaussian 09 software [31].

2.2. Hyperfine Coupling Constant (HFCC) Calculations. After MD simulations, the structures of Complexes **1** and **2** (Figure 1) with water molecules were used for the hyperfine coupling constant (HFCC) calculations. For both complexes, the A_{iso} calculations were performed using the functional PBE1PBE [32] with the basis set aug-cc-pVTZ-J and EPR-III [33] for hydrogen and oxygen atoms; 6-31G [34] for the carbon, and nitrogen and sulfur atoms and LanL2dz for the technetium atom in the Gaussian 09 program [31]. For the discussions of A_{iso} calculations, we used the following notation: level of A_{iso} computation//level of geometry optimization or MD simulation. For example: (PBE1PBE (H_2O)//BP86 (H_2O)) means A_{iso} computation with explicit solvent//geometry optimization with explicit solvent; (PBE1PBE (H_2O)/PCM//BP86 (H_2O)) means A_{iso} computation with explicit

and implicit solvent (PCM)//geometry optimization with explicit solvent molecules.

The (PBE1PBE (H_2O)//BP86 (H_2O)) structures were used as the starting point for the MD simulations. The same notation is utilized when including the dynamic effect (MD simulation).

2.3. QTAIM Calculations and Spin Density Distributions. The *Quantum Theory of Atoms in Molecules* (QTAIM) is firstly an extension of quantum mechanics to subdomains, properly defining an atom as an open system. The QTAIM is important to describe the properties of atoms (such as the nature of the chemical bond and the strength of hydrogen bonding) [35, 36]. AIM analysis was performed using calculations in the AIMALL [37] and QTAIMQB program [36], the analysis of the results were made by the AIMSTUDIO program [37], and both are part of the AIMALL program package [37].

The QTAIM calculations were performed with the optimized geometries at the level BP86/Lanl2dz. Atomic spin density was evaluated using the natural population analysis (NPA) performed in the Gaussian 09 program [31]; the contour surface was fixed at 0.0004 a.u value.

3. Results and Discussion

3.1. Validation of the Hyperfine Coupling Constant (HFCC) Calculations. This stage of the work was performed to validate the theoretical methodology used to calculate the EPR parameters, because, to our knowledge, there is no ^{1}H and [17]O hyperfine coupling constant data for the proposal complexes in Figure 1 reported in the literature so far.

It is known that the relaxation theory of NMR has been the subject of many books and scientific articles [38]. Thus, the NMR relaxation parameters have been considered one of the most useful and versatile methods for the investigation of MRI probes. The relaxation time (T_1 and T_2) is given by paramagnetic ions that are able to interact with the water molecules, drastically reducing the relaxation times. Equations (1) show the relaxation times T_1 and T_2 induced by paramagnetic ions in aqueous solution, respectively [39, 40]:

$$R_1 = \frac{1}{T_1}$$
$$\cong \frac{1}{15} \frac{S(S+1) g_e^2 \beta^2 g_N^2 \beta_N^2}{\hbar^2 r^6}$$
$$+ \left(\frac{A}{\hbar}\right)^2 \frac{S(S+1)}{3} \left[\frac{2\tau_e}{1+(\omega_I \tau_e)^2}\right]$$

$$R_2 = \frac{1}{T_2}$$
$$\cong \frac{1}{15} \frac{S(S+1) g_e^2 \beta^2 g_N^2 \beta_N^2}{\hbar^2 r^6}$$
$$+ \left(\frac{A}{\hbar}\right)^2 \frac{S(S+1)}{3} \left[\tau_c + \frac{\tau_c}{1+(\omega_S \tau_e)^2}\right]$$

(1)

The relaxation time constant (T_1 and T_2) depends on the electron spin (S), the electronic and proton g factors (g_e and g_N, resp.), the Bohr magnet on (β), the nuclear magnet on (β_N), the hyperfine coupling constant (A), the ion-nucleus distance (r), and the Larmor frequencies for the proton and electron spins (ω_I and ω_S, resp.). The correlation times τ_c and τ_e are characteristic of the rate of change of the interactions between the metallic species and neighboring protons. In fact, the order parameter, the overall molecular rotational correlation time (τ_c), and the internal rotational correlation time (τ_e) are essential motional parameters to obtain pictures of molecular motion [39, 40]. In (1), each of the relaxation rates (R_1 and R_2) is a sum of two terms. The first term comes from the dipolar coupling and the second term from the scalar coupling [39, 40].

In order to validate our calculation strategy for ^{1}H and [17]O hyperfine coupling constant values, the complex $[Mn(H_2O)_6]^{2+}$ was used [41–43]. In this line, theoretical and experimental values are reported in Table 1. The theoretical calculations were performed using two different basis sets (EPR-III and aug-cc-pVTZ-J) with the functional PBE1PBE. Among other basis sets, the choice of the basis sets EPR-III and aug-cc-pVTZ-J with the functional PBE1PBE improved the results, so that they are completely satisfactory. Both basis sets have been shown to be satisfactory in similar structures [31, 41, 42]. The smaller basis sets are unsatisfactory and the larger are too expensive.

For the HFCCs calculations of the static equilibrium structure in the presence of explicit solvent A_{iso}^{eq} ((PBE1PBE (H_2O)//BP86 (H_2O)), we obtained 0.62 and 0.76 MHz for ^{1}H and values of 1.98 and 3.14 MHz for [17]O at the EPR-III and aug-cc-pVTZ-J levels, respectively. For the static equilibrium structure with explicit and implicit solvent A_{iso}^{eq} (PBE1PBE(H_2O)/PCM//BP86 (H_2O)), the values 0.23 and 0.66 MHz for ^{1}H and 2.08 and 1.41 MHz were obtained for [17]O at the EPR-III and aug-cc-pVTZJ levels, respectively. Taking into consideration now the structures selected during the MD simulation, $A_{iso}^{310 K}$ (MD(H_2O)//MD(H_2O)), values of 0.81 and 1.00 MHz for ^{1}H and 2.23 and 4.96 MHz for [17]O, with the basis set EPR-III and aug-cc-pVTZ-J, were obtained, respectively. The experimental values for $[Mn(H_2O)_6]^{2+}$ are 0.81 and 5.38 MHz for ^{1}H and [17]O, respectively. Thus, it is possible to observe that the aug-cc-pVTZ-J basis set is in much better agreement with the experimental values; on the other hand, the [17]O values at the EPR-III level are far from the experimental value.

3.2. Thermal and Solvent Effects on the Hyperfine Coupling Constant (HFCC) for Complex 1. According to Tzanopoulou et al., Figure 1 is a potential candidate for imaging techniques (^{99m}Tc), facilitating breast cancer diagnosis [12, 13]. In view of that, we have performed EPR calculations evaluating thermal and solvent effects on the hyperfine coupling constant (HFCC) in Complex **1**.

In Table 2, it is possible to observe that the A_{iso}^{eq} values for the static equilibrium structure with the explicit solvent ((PBE1PBE (H_2O)//BP86 (H_2O)) were 0.89 and 3.39 MHz

Table 1: Calculated hyperfine coupling constants (A_{iso}) [MHz] for static equilibrium structure (A_{iso}^{eq}) and for the structures selected during the MD simulation ($A_{iso}^{310\,K}$).

$[Mn(H_2O)_6]^{2+}$ A_{iso} Type	Method	^1H [MHz][b]	^{17}O [MHz][b]
A_{iso}^{eq} (PBE1PBE (H_2O)//BP86 (H_2O))	EPR-III	0.62	1.98
	AUG-cc-pVTZ-J	0.76	3.14
A_{iso}^{eq} (PBE1PBE(H_2O)/PCM//BP86 (H_2O))	EPR-III	0.23	2.08
	AUG-cc-pVTZ-J	0.66	1.41
$A_{iso}^{310\,K}$ (MD(H_2O)//MD(H_2O))[c]	EPR-III	0.81 ± 0.10[a]	2.23 ± 0.83[a]
	AUG-cc-pVTZ-J	1.00 ± 0.10[a]	4.96 ± 0.90[a]
Experimental[40]		*0.81*	*5.38*

[a]Standard deviations values. [b]A_{iso} values for ^{17}O and ^1H correspond to average values for all water molecules present in the system. [c]A_{iso} average values for the 40 conformations selected of MD.

Table 2: Calculated hyperfine coupling constants (A_{iso}) [MHz] for static equilibrium structure (A_{iso}^{eq}) and for the structures selected during the MD simulation ($A_{iso}^{310\,K}$) with aug-cc-pVTZ-J level.

Complex **1**	A_{iso}	
Type	^1H [MHz][b]	^{17}O [MHz][b]
A_{iso}^{eq} (PBE1PBE(H_2O)//BP86 (H_2O))	0.89	3.39
A_{iso}^{eq} (PBE1PBE(H_2O)/PCM//BP86 (H_2O))	0.84	3.79
$A_{iso}^{310\,K}$ (MD(H_2O)//MD(H_2O))[c]	1.07 ± 0.16[a]	1.50 ± 0.65[a]

[a]Standard deviations values. [b]A_{iso} values for ^{17}O and ^1H correspond to average values for all water molecules present in the system. [c]A_{iso} average values for the 40 conformations selected of MD.

for ^1H and ^{17}O, respectively. For the static equilibrium structure with explicit and implicit solvent A_{iso}^{eq} (PBE1PBE(H_2O)/PCM//BP86(H_2O)), we obtained ^1H and ^{17}O values of 0.84 for 3.79 MHz, respectively. A slight difference was observed between the implicit and explicit/implicit solvent of 0,05 MHz for the ^1H and 0,4 MHz for ^{17}O (Table 2). This small difference between the explicit and explicit/implicit solvent is to be expected, which shows that the number of water molecules added during the A_{iso} calculation describes the system well. Considering now the structures selected during the MD simulation, $A_{iso}^{310\,K}$ (MD(H_2O)//MD(H_2O)), values of 1.07 and 1.50 MHz were obtained for ^1H and ^{17}O, respectively. Thus, it can be seen that the thermal effects greatly influence the system, particularly the water molecule ^{17}O atoms, as can be seen in Table 2.

It is important to observe in Table 2 that the A_{iso}^{eq} and $A_{iso}^{310\,K}$ values for Complex **1** are higher than the gadolinium complex in solution, which is the most used contrast agent currently. According to the literature, the A_{iso} experimental values for $[GdL(H_2O)]^{n+/-} \times H_2O$ complexes can vary between 0.5 and 0.6 MHz [44, 45].

It should be kept in mind, however, that the use of gadolinium complexes as MRI contrast agents has revealed serious problems due to their high toxicity [46]. Based on this context, an alternative is the use of technetium complexes as MRI contrast agents, which present lower toxicity and show good (A_{iso}) results in solution (see Table 2).

3.3. Thermal and Solvent Effects on the Hyperfine Coupling Constant (HFCC) for Complex 2. In this work, we have also

performed EPR calculations, evaluating thermal and solvent effects on the Hyperfine Coupling Constants (HFCCs) on Complex **2** (Figure 1), in order to investigate also the influence of the Tc coordination environments on the A_{iso} values.

In Table 3, it is possible to observe that, for the static equilibrium structure with the explicit solvent A_{iso}^{eq} (PBE1PBE(H_2O)//BP86 (H_2O)), the values 1.28 MHz for ^1H and 2.30 MHz for ^{17}O were obtained. For the static equilibrium structure with explicit and implicit solvent A_{iso}^{eq} (PBE1PBE(H_2O)/PCM//BP86 (H_2O)) the values 1.02 MHz for ^1H and 2.40 MHz for ^{17}O were obtained. Thus, there is a small difference between both solvation models (explicit and explicit/implicit solvents) of 0.26 MHz and 0.10 MHz for ^1H and ^{17}O, respectively. It is possible to notice that explicit water molecules are sufficient to realistically represent our system.

By analyzing the structures selected during the MD simulation, $A_{iso}^{310\,K}$ (MD(H_2O)//MD(H_2O)), the ^1H and ^{17}O values of 1.41 and 2.78 MHz were obtained, respectively. Thus, it can be seen that the thermal effects are very important for spectroscopic calculations.

It is important to observe that the Tc coordination environments are different for both complexes, $Tc(CO)_3(NNO)$ and $[Tc(NO)(aha)_2(H_2O)]^+$, Complex **1** and **2**, respectively. For equilibrium geometry, comparing the A_{iso} values for Complex **1** (Table 2) with Complex **2** (Table 3), the changes in the A_{iso}^{eq} values for ^{17}O were up to 1.09 MHz. On the other hand, the changes in the A_{iso}^{eq} values for ^1H were up to 0.39 MHz. Also it is important to notice that when the thermal effect was included in system, a difference was observed in the $A_{iso}^{310\,K}$ values of 1.28 and 0.34 MHz for the ^{17}O and ^1H atoms, respectively (see Tables 2 and 3). Based on this context,

TABLE 3: Calculated hyperfine coupling constants (A_{iso}) [MHz] for static equilibrium structure (A_{iso}^{eq}) and for the structures selected during the MD simulation ($A_{iso}^{310\,K}$) with aug-cc-pVTZ-J level.

Complex **2**	A_{iso}	
Type	^{1}H [MHz][b]	^{17}O [MHz][b]
A_{iso}^{eq} (PBE1PBE(H$_2$O)//BP86 (H$_2$O))	1.28	2.30
A_{iso}^{eq} (PBE1PBE(H$_2$O)/PCM//BP86 (H$_2$O))	1.02	2.40
$A_{iso}^{310\,K}$ (MD(H$_2$O)//MD(H$_2$O))[c]	1.41 ± 0.14[a]	2.78 ± 0.31[a]

[a]Standard deviations values. [b]A_{iso} values for ^{17}O and ^{1}H correspond to average values for all water molecules present in the system. [c]A_{iso} average values for the 40 conformations selected of MD.

TABLE 4: QTAIM parameters obtained at the hydrogen bond BCPs for the structures of **1**-**2**(au) (structures 1: Complex **1** with water and 2: Complex **2** with water molecules).

Structure	$\rho(r)$	$\nabla^2\rho(r)$	ε	$V(r)$	$G(r)$	$H(r)$
1a$_{(Oa\cdots Ha)}$	+0.033326	+0.120236	+0.149635	−0.031505	+0.030782	−0.000723
1b$_{(Ob\cdots Hb)}$	+0.027099	+0.099372	+0.057624	−0.023879	+0.024361	+0.000482
1c$_{(Na\cdots Hc)}$	+0.014533	+0.049406	+0.477539	−0.009003	+0.010677	+0.001674
2a$_{(Oa\cdots Ha)}$	+0.027257	+0.115545	+0.083698	−0.025766	+0.027326	+0.00156
2b$_{(Ob\cdots Hb)}$	+0.019167	+0.076374	+0.094193	−0.015995	+0.017544	+0.001549
2c$_{(Oc\cdots Hc)}$	+0.010155	+0.040305	+0.230208	−0.006249	+0.008162	+0.001913

our findings point out that changes in the coordination environment of Tc complexes can significantly influence the A_{iso} results.

3.4. Analysis of Quantum Theory of Atoms in Molecules (QTAIM) and Spin Density Distributions.

The QTAIM methodology is a quantum model considered innovative in studies of chemical bonds but also is effective in characterizing intramolecular and/or intermolecular interactions [47]. Thus, QTAIM calculations are very important to check the influence of hydrogen bonds in the A_{iso} values [40–52]; this model was developed by Bader [48]. Table 4 shows the values of the analyzed parameters **1a**, **1b**, **1c** (Complex **1**) and **2a**, **2b**, **2c** (Complex **2**) are the interactions analyzed for. According to the Koch and Popelier parameter [49], the atoms in **1a** possess $\nabla^2\rho(r) > 0$ and $H(r) < 0$, suggesting partial covalent interactions. Now, the other analyzed interactions (1a, 1b, 1c, 2a, 2b, and 2c) possess $\nabla^2\rho(r) > 0$ and $H(r) > 0$, suggesting noncovalent interactions.

From the rigorous concepts of QTAIM, the BCPs (bond critical points) are located on hydrogen bonds formed by proton donors and electrons π, Figures 2(b) and 3 [34, 44]; thus the low $\rho(r)$ values along with the positive results of the Laplacian ($\nabla^2\rho(r)$) indicate the formation of hydrogen bonds in each intermolecular BCP. Thus, we can see that when putting the water molecules in the system, interactions of free water molecules with the oxygen of complex (HO$\cdots$H) can take place.

Interestingly, some hydrogen bonds (HO$\cdots$H) among free water molecules in solution were broken and new hydrogen bonds taken place with the complex, thereby conferring extra stability to the system.

Figure 4 shows the spin density around the atoms complex; the distribution of the spin density in a given paramagnetic molecule indicates the contributions due to electrons
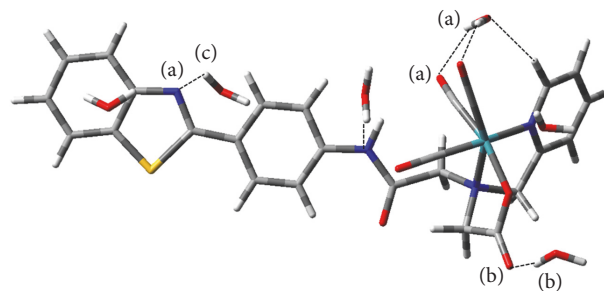

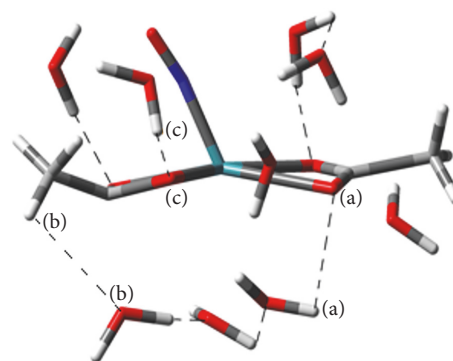FIGURE 2: Geometry for Complex **1** with water molecules.

FIGURE 3: Geometry for Complex **2** with water molecules.

with the majority spin (α) and the minority spin (β) [50, 51]. In Figure 4 these regions are represented by the colors blue (spin α) and green (spin β). Thus, Figure 4 shows a high spin density around the complex, especially the part around the metal and it is possible to note that there electron transfer from the metal (spin α) to the ligands of the complex (spin β). A characteristic indication of a spin-polarization effect is

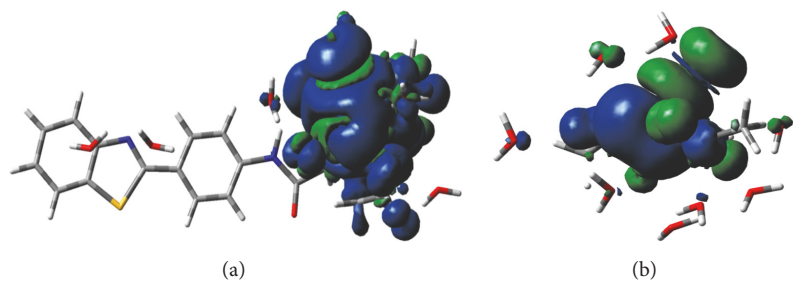(a)   (b)

FIGURE 4: Spin density map of the compounds (the isosurface contour value is 0.0004). (a) Complex **1**; (b) Complex **2**.

the presence of alternate spin density signs along the pathway of the bonded atoms radiating out from the paramagnetic atom. For our complex, the density is negative around the ^{17}O nucleus of coordinated water molecules and positive at their ^{1}H nuclei. Thus, the significant increase of A_{iso} values is due to the strong hydrogen bonding of water molecules with the complex and also due to the transfer of electrons around the complex [52].

4. Conclusions

In this work, the performance of two basis sets, EPR-III and aug-cc-pVTZ-J, was evaluated in $[\text{Mn}(\text{H}_2\text{O})_6]^{2+}$ in ^{17}O and ^{1}H HFCCs calculations. Our results show that the aug-cc-pVTZ-J bases set presents a realistic description of the system ($[\text{Mn}(\text{H}_2\text{O})_6]^{2+}$) in different environments, because good agreement was observed between theoretical and experimental results for A_{iso} values.

Furthermore, it was possible to theoretically determine the A_{iso} values for ^{17}O and ^{1}H in Complexes **1** and **2**. Thermal and solvent effects were also studied computationally by quantum-chemical methods. It is worth noting that these effects are important for ^{17}O and ^{1}H HFCC calculations.

It is well-known that the use of gadolinium complexes as MRI contrast agents has generated several problems due to their high toxicity [9]. However, our theoretical findings point out that an alternative to this traditional approach is to use technetium complexes as MRI contrast agents. They present lower toxicity and show good A_{iso} results in solution. Motivated by this idea, we report a theoretical proof-of-principle study on the use of Tc complexes for designing new MRI probes. To our knowledge, this is the first application of this approach in the condensed phase.

Conflicts of Interest

The authors declare that they have no conflicts of interest.

Acknowledgments

References

[1] B. Dunn, "Cancer: Solving an age-old problem," *Nature*, vol. 483, no. 7387, pp. S2–S6, 2012.

[2] E. R. Galvão, L. M. Martins, J. O. Ibiapina, H. M. Andrade, and S. J. Monte, "Breast cancer proteomics: a review for clinicians," *Journal of Cancer Research and Clinical Oncology*, vol. 137, no. 6, pp. 915–925, 2011.

[3] A. Jemal, R. Siegel, J. Xu, and E. Ward, "Cancer statistics," *CA Cancer Journal for Clinicians*, vol. 60, no. 5, pp. 277–300, 2010.

[4] C. D. Angelis, R. F. Brizzi, and R. Pellicano, "Endoscopic ultrasonography for pancreatic cancer: Current and future perspectives," *Journal of Gastrointestinal Oncology*, vol. 4, no. 2, pp. 220–230, 2013.

[5] L. F. Chala and N. Barros, "Avaliação das mamas com métodos de imagem," *Radiologia Brasileira*, vol. 40, no. 1, pp. 4–6, 2007.

[6] A. A. Mazzola, "Ressonância magnética: princípios de formação da imagem e aplicações em imagem funcional," *Revista Brasileira de Física Médica*, vol. 3, pp. 117–129, 2009.

[7] G. H. Im, S. M. Kim, D.-G. Lee, W. J. Lee, J. H. Lee, and I. S. Lee, "Fe3O4/MnO hybrid nanocrystals as a dual contrast agent for both T(1)- and T(2)-weighted liver MRI," *Biomaterials*, vol. 34, no. 8, pp. 2069–2076, 2013.

[8] P. Caravan, J. J. Ellison, T. J. McMurry, and R. B. Lauffer, "Gadolinium(III) chelates as MRI contrast agents: structure, dynamics, and applications," *Chemical Reviews*, vol. 99, no. 9, pp. 2293–2352, 1999.

[9] M. Sagnou, S. Tzanopoulou, C. P. Raptopoulou et al., "A phenylbenzothiazole conjugate with the tricarbonyl fac-[M(I)(CO)$_3$] + (M = Re, ^{99}Tc, ^{99m}Tc) core for imaging of β-Amyloid plaques," *European Journal of Inorganic Chemistry*, no. 27, pp. 4279–4286, 2012.

[10] V. P. Tarasov, Y. B. Muravlev, K. E. German, and N. N. Popova, "^{99}Tc NMR of Supported Technetium Nanoparticles," *Doklady Physical Chemistry*, vol. 377, pp. 71–76, 2001.

[11] D. T. Mancini, E. F. Souza, M. S. Caetano, and T. C. Ramalho, "99Tc NMR as a promising technique for structural investigation of biomolecules: Theoretical studies on the solvent and thermal effects of phenylbenzothiazole complex," *Magnetic Resonance in Chemistry*, vol. 52, no. 4, pp. 129–137, 2014.

[12] S. Tzanopoulou, I. C. Pirmettis, G. Patsis et al., "Synthesis, characterization, and biological evaluation of M(I)(CO) 3(NNO) complexes (M = Re, 99mTc) conjugated to 2-(4-aminophenyl)benzothiazole as potential breast cancer radiopharmaceuticals," *Journal of Medicinal Chemistry*, vol. 49, no. 18, pp. 5408–5410, 2006.

[13] S. Tzanopoulou, M. Sagnou, M. Paravatou-Petsotas et al., "Evaluation of Re and 99mTc complexes of 2-(4′-aminophenyl) benzothiazole as potential breast cancer radiopharmaceuticals," *Journal of Medicinal Chemistry*, vol. 53, no. 12, pp. 4633–4641, 2010.

[14] D.-F. Shi, T. D. Bradshaw, S. Wrigley et al., "Antitumor benzothiazoles. 3. Synthesis of 2-(4- aminophenyl)benzothiazoles and evaluation of their activities against breast cancer cell lines in vitro and in vivo," *Journal of Medicinal Chemistry*, vol. 39, no. 17, pp. 3375–3384, 1996.

[15] D. T. Mancini, K. Sen, M. Barbatti, W. Thiel, and T. C. Ramalho, "Excited-state proton transfer can tune the color of protein fluorescent markers," *ChemPhysChem*, vol. 16, no. 16, pp. 3444–3449, 2015.

[16] U. Abram and R. Alberto, "Technetium and rhenium—coordination chemistry and nuclear medical applications," *Journal of the Brazilian Chemical Society*, vol. 17, no. 8, pp. 1486–1500, 2006.

[17] N. I. Gorshkov, A. A. Lumpov, A. E. Miroslavov, V. A. Mikhalev, and D. N. Suglobov, "99Tc NMR study of complexation of [Tc(CO)3(H2O)3]+ with halide and thiocyanate ions in aqueous solutions," *Czechoslovak Journal of Physics*, vol. 53, pp. A745–A749, 2003.

[18] K. J. Franklin, C. J. L. Lock, B. G. Sayer, and G. J. Schrobilgen, "Chemical applications of 99Tc NMR spectroscopy: preparation of novel Tc(VII) species and their characterization by multinuclear NMR spectroscopy," *Journal of the American Chemical Society*, vol. 104, no. 20, pp. 5303–5306, 1982.

[19] S. S. Jurisson and J. D. Lydon, "Potential technetium small molecule radiopharmaceuticals," *Chemical Reviews*, vol. 99, no. 9, pp. 2205–2218, 1999.

[20] S. M. Balasekaran, J. Spandl, A. Hagenbach, K. Köhler, M. Drees, and U. Abram, "Fluoridonitrosyl complexes of technetium(I) and technetium(II). synthesis, characterization, reactions, and DFT calculations," *Inorganic Chemistry*, vol. 53, no. 10, pp. 5117–5128, 2014.

[21] A. D. Becke, "Density-functional exchange-energy approximation with correct asymptotic behavior," *Physical Review A*, vol. 38, no. 6, pp. 3098–3100, 1988.

[22] J. P. Perdew, "Density-functional approximation for the correlation energy of the inhomogeneous electron gas," *Physical Review B*, vol. 33, no. 12, pp. 8822–8824, 1986.

[23] J. P. Perdew, "Erratum: Density-functional approximation for the correlation energy of the inhomogeneous electron gas," *Physical Review B*, vol. 34, no. 10, p. 7406, 1986.

[24] T. H. Dunning Jr. and P. J. Hay, "Methods of Electronic Structure Theory," in *Modern Theoretical Chemistry*, H. F. Schaefer, Ed., vol. 3, pp. 1–28, Plenum Press, New York, NY, USA, 3rd edition, 1977.

[25] S. S. Iyengar, H. B. Schlegel, and G. A. Voth, "Atom-centered density matrix propagation (ADMP): Generalizations using Bohmian mechanics," *Journal of Physical Chemistry A*, vol. 107, no. 37, pp. 7269–7277, 2003.

[26] D. Van der, A. R. Spoel, E. Apol et al., *GROMACS User Manual*, version 3.0, 2001.

[27] A. P. Guimarães, A. A. Oliveira, E. F. F. Da Cunha, T. C. Ramalho, and T. C. C. França, "Analysis of Bacillus anthracis nucleoside hydrolase via in silico docking with inhibitors and molecular dynamics simulation," *Journal of Molecular Modeling*, vol. 17, no. 11, pp. 2939–2951, 2011.

[28] T. C. Ramalho and M. Bühl, "Probing NMR parameters, structure and dynamics of 5-nitroimidazole derivatives. Density functional study of prototypical radiosensitizers," *Magnetic Resonance in Chemistry*, vol. 43, no. 2, pp. 139–146, 2005.

[29] T. C. Ramalho, D. H. Pereira, and W. Thiel, "Thermal and solvent effects on NMR indirect spin - Spin coupling constants of a prototypical chagas disease drug," *Journal of Physical Chemistry A*, vol. 115, no. 46, pp. 13504–13512, 2011.

[30] M. A. Gonçalves, L. S. Santos, D. M. Prata, F. C. Peixoto, E. F. da Cunha, and T. C. Ramalho, "Optimal wavelet signal compression as an efficient alternative to investigate molecular dynamics simulations: application to thermal and solvent effects of MRI probes," *Theoretical Chemistry Accounts*, vol. 136, no. 1, pp. 2–13, 2017.

[31] M. J. Frisch, G. W. Trucks, H. B. Schlegel et al., *Gaussian 09, Revision C.02*, Gaussian, Inc, 2004.

[32] J. P. Perdew, K. Burke, and M. Ernzerhof, "Generalized gradient approximation made simple," *Physical Review Letters*, vol. 77, no. 18, pp. 3865–3868, 1996.

[33] E. D. Hedegård, J. Kongsted, and S. P. A. Sauer, "Improving the calculation of electron paramagnetic resonance hyperfine coupling tensors for d-block metals," *Physical Chemistry Chemical Physics*, vol. 14, no. 30, pp. 10669–10676, 2012.

[34] R. Ditchfield, W. J. Hehre, and J. A. Pople, "Self-consistent molecular-orbital methods. IX. An extended gaussian-type basis for molecular-orbital studies of organic molecules," *The Journal of Chemical Physics*, vol. 54, no. 2, pp. 720–723, 1971.

[35] F. Cortés-Guzmán and R. F. W. Bader, "Complementarity of QTAIM and MO theory in the study of bonding in donor-acceptor complexes," *Coordination Chemistry Reviews*, vol. 249, no. 5-6, pp. 633–662, 2005.

[36] R. F. W. Bader, "Principle of stationary action and the definition of a proper open system," *Physical Review B*, vol. 49, no. 19, pp. 13348–13356, 1994.

[37] T. A. Keith, AIM ALL (version 10.05.04), TK Gristmill Software, Overland Park KS, 2010.

[38] M. Kaupp, M. Bühl, V. V. G. Malkin, (Eds.). Weinheim432, 2004.

[39] M. Lepage and J. C. Gore, "Contrast mechanisms in magnetic resonance imaging," *Journal of Physics*, vol. 3, pp. 78–86, 2004.

[40] O. V. Yazyev, L. Helm, V. G. Malkin, and O. L. Malkina, "Quantum chemical investigation of hyperfine coupling constants on first coordination sphere water molecule of gadolinium(III) aqua complexes," *Journal of Physical Chemistry A*, vol. 109, no. 48, pp. 10997–11005, 2005.

[41] M. A. Goncalves, E. F. F. da Cunha, F. C. Peixoto, and T. C. Ramalho, "Probing thermal and solvent effects on hyperfine interactions and spin relaxation rate of δ-FeOOH(100) and [MnH₃buea(OH)]$^{2-}$: toward new MRI probes," *Computational and Theoretical Chemistry*, vol. 1069, pp. 96–104, 2015.

[42] M. A. Goncalves, E. F. F. da Cunha, F. C. Peixoto, and T. C. Ramalho, "NMR parameters and hyperfine coupling constants of the Fe₃O₄(100)-water interface: implications for MRI probes," *Chemical Physics Letters*, vol. 609, pp. 88–92, 2014.

[43] G. A. Rolla, C. Platas-Iglesias, M. Botta, L. Tei, and L. Helm, "1H and 17O NMR relaxometric and computational study on macrocyclic Mn(II) complexes," *Inorganic Chemistry*, vol. 52, no. 6, pp. 3268–3279, 2013.

[44] D. H. Powell, O. M. Ni Dhubhghaill, D. Pubanz et al., "Structural and dynamic parameters obtained from 17O NMR, EPR, and NMRD studies of monomeric and dimeric Gd3+ complexes of interest in magnetic resonance imaging: an integrated and theoretically self-consistent approach," *Journal of the American Chemical Society*, vol. 118, no. 39, pp. 9333–9346, 1996.

[45] S. Laurent, L. V. Elst, S. Houzé, N. Guérit, and R. N. Muller, "Synthesis and characterization of various benzyl diethylene-triaminepentaacetic acids (dtpa) and their paramagnetic complexes, potential contrast agents for magnetic resonance imaging," *Helvetica Chimica Acta*, vol. 83, no. 2, pp. 394–406, 2000.

[46] K. Kattel, J. Y. Park, W. Xu et al., "Paramagnetic dysprosium oxide nanoparticles and dysprosium hydroxide nanorods as T_2 MRI contrast agents," *Biomaterials*, vol. 33, no. 11, pp. 3254–3261, 2012.

[47] B. G. Oliveira, R. C. Araújo, and M. N. Ramos, "A topologia molecular QTAIM e a descrição mecânico-quântica de ligações de hidrogênio e ligações de di-hidrogênio," *Química Nova*, vol. 33, no. 5, pp. 1155–1162, 2010.

[48] R. F. W. Bader, *Atoms in Molecules-A Quantum Theory*, Oxford University Press, Oxford, U.K, 1990.

[49] M. Pecul, J. Lewandowski, and J. Sadlej, "Benchmark calculations of the shielding constants in the water dimer," *Chemical Physics Letters*, vol. 333, no. 1-2, pp. 139–145, 2001.

[50] D. Esteban-Gõmez, A. De Blas, T. Rodríguez-Blas, L. Helm, and C. Platas-Iglesias, "Hyperfine coupling constants on inner-sphere water molecules of Gd III-based MRI contrast agents," *ChemPhysChem*, vol. 13, no. 16, pp. 3640–3650, 2012.

[51] E. Ruiz, J. Cirera, and S. Alvarez, "Spin density distribution in transition metal complexes," *Coordination Chemistry Reviews*, vol. 249, no. 23, pp. 2649–2660, 2005.

[52] E. Alarcón, M. González-Béjar, S. Gorelsky et al., "Photophysical characterization of atorvastatin (Lipitor®) ortho-hydroxy metabolite: Role of hydroxyl group on the drug photochemistry," *Photochemical and Photobiological Sciences*, vol. 9, no. 10, pp. 1378–1384, 2010.